Transactions of the **13th International Conference on Structural Mechanics in Reactor Technology** (SMiRT 13), Escola de Engenharia - Universidade Federal do Rio Grande do Sul, Porto Alegre, Brazil, August 13-18, 1995

Analysis of FVT of the Hualien LSST model using a flexible volume substructuring method

Nakamura, N.
Tokyo Electric Power Company, Tokyo, Japan
Tang, H.T.
Eletric Power Research Institute, Palo Alto, CA, U.S.A.

ABSTRACT: Post-test correlation analyses of forced vibration tests of the Hualien Large Scale Seismic Test Containment Model were performed using a three-dimensional flexible volume substructuring method. The modeling effects and soil property sensitivities were evaluated. The computed resonance and phase lag curves were compared with the test results. In general, where a thin layer of softer soil was considered beneath the basemat and around the structure, the analysis results matched well with the test data. To get better correlation of the model deformation, the stiffness of the containment model had to be softened.

1 INTRODUCTION

A 1/4-scale cylindrical reactor containment model was constructed in Hualien, Taiwan for soil-structure interaction (SSI) effect evaluation and SSI analysis procedure verification (Tang et al. 1991). Forced vibration tests (FVT) were executed before backfill (FVT-1) and after backfill (FVT-2) to characterize soil-structure system characteristics under low excitations (Morishita et al. 1993 and Sugawara et al. 1995a). A number of organizations participated in the pre-test blind prediction and post-test correlation analyses of the forced vibration test using various industry familiar methods.

In the current study, correlation analyses were performed using a three-dimensional flexible volume substructuring method (The SASSI development team 1988). To achieve best correlation, soil properties were parametrically varied. It was found that the analysis results agreed well with the test results if a softer soil layer around and beneath the super-structure foundation was assumed (Tang and Nakamura 1995). In this paper, further studies considering variations of structure properties are reported.

2 FVT TEST

2.1 *Forced vibration test*

The 1/4-scale containment model as shown in Figure 1 is a cylindrical reinforced concrete structure about 16 m high. The diameter is about 11 m and the total weight is about 1,460 tonf. Approximately one-third of the model, 5 m depth, is embedded after the backfill.

In both FVT-1 and FVT-2, the first floor and roof floor were excited along the north-south (NS) and east-west (EW) directions. Since the test results and geotechnical investigations showed that the soil conditions in the field exhibited minor anisotropy due to inhomogeneity, response resonance curves along the two principal axes, D1 and D2, were deduced by transposing the NS and EW direction test results (Morishita et al. 1993 and Sugawara et al. 1995a). The peak frequencies are 4.1 Hz along the D1 direction and 4.6 Hz along D2 for FVT-1. For FVT-2, the peak frequencies are 6.1 Hz along D1 and 6.3 Hz along D2 showing smaller anisotropy after backfill.

2.2 *Evaluation of soil condition*

For blind prediction, unified soil models (Kokusho et al. 1993) based on soil investigation results were prescribed for all participants. For FVT-1, two unified models, line-A and line-B, were recommended. In general, the unified models yielded higher peak frequencies comparing with the test results (Tang and Nakamura 1995). To assess why the prediction results gave higher frequencies, the in-situ soil condition was evaluated using impedance functions. Figure 2 compares impedance functions based on the unified soil models (in solid lines) with those back-calculated from the D1 and D2 results of FVT-1. From the figure, the following are noticed:

1) Real part calculated based on the unified soil model line-B is much larger than the back-calculated one.

2) Real part based on line-A is slightly larger than the back-calculated.

3) Real part of the D2 direction impedance is larger than that of D1. This trend corresponds with the difference of the calculated peak frequencies along the two principal directions.

3 CORRELATION ANALYSIS

3.1 *Analysis condition*

In the current study, anisotropy was ignored and the analysis results represent averaged isotropic conditions. The analysis results were compared with the transposed D1 and D2 direction test results. As discussed in section 2.2, the actual soil conditions for FVT-1 were inferred to be softer than the unified models suggested. Regarding the cause, it was judged that soil material non-linearity was negligible, since the exciting force level was low. Instead, the cause may be due to a softer soil layer surrounding the containment model. The basis of the softer layer assumption is that the original overburden stress condition of the soil was released by excavation works.

In the previous study (Tang and Nakamura 1995), parametric analyses were performed by assuming several different soil conditions for FVT-1 and FVT-2. The best estimated models, for FVT-1, a softer soil layer assumed beneath the basemat, and for FVT-2, a softer soil layer added around the embedment part of the structure, yielded results matching well with the test results. However, the calculated model peak amplitude and the ratio of the elastic deformation component were slightly lower. (The total roof top response of the model is composed of three components, rocking, swaying and elastic deformation.) Sugawara et al. (1995b) related these discrepancies to the model concrete structural stiffness. In line with their findings, further correlation analyses as described below were performed by modifying the structure model properties.

3.2 *Analysis model*

Figure 3 shows the analysis model. For FVT-1, the super-structure sitting in a pit was assumed to be free-standing on a half space composed of horizontal-layered gravelly soils. The surrounding alluvium above the super-structure foundation which was not in contact with the structure was neglected. The super-structure was modeled with lumped-masses and three-dimensional beam, shell and solid elements. For FVT-2, the backfill soil and the excavated soil were modeled with three-dimensional solid elements.

The structure and soil properties are given in Tables 1 and 2, respectively. Case-A in the tables corresponds to the best estimated model of the previous study (Tang and Nakamura 1995) in which the structure properties are the prescribed ones based on concrete cylinder specimen testing and design drawings. Case-B considers that the structure model properties were modified following the Sugawara et al. (1995b) suggestions. In their study, Young's modulus of the shell wall was uniformly softened based on the test results. However, in the current study, two Young's moduli were applied for upper and lower parts of the shell wall taking into account the model construction condition. Further, geometrical coefficient for shear deformation was revised. The fixed-base first natural frequency of case-A was 10.1 Hz and one of case-B was 9.31 Hz. As for the soil foundation configuration, a softer soil layer was assumed beneath the basemat for FVT-1 and added around the embedment part of the structure for FVT-2.

3.3 *Analysis result*

The calculated resonance and phase lag curves are compared with the principal direction test results as shown in Figure 4 for location H15 on the roof floor for the roof floor excitation of FVT-1. White and black circles express the transposed results of D1 and D2 directions. Figure 5 shows those of FVT-2. Table 3 gives peak frequencies and damping factors obtained from the resonance curves at H15 and also ratios of each deformation component. From these results, the following are observed:

1) Both case-A and case-B yield peak frequencies and shape of resonance and phase lag curves matching well the test results.

2) Comparison of the case-A results with those of case-B indicates that the modified structure model response has larger elastic component and smaller rocking component. The calculated deformation ratio thus matches better that of the test results.

4 CONCLUSION

Parametric correlation studies of the forced vibration tests were performed using a flexible volume substructuring method. The computed resonance and phase lag curves agreed well with the test results if one assumes soft soil in contact with the model and lower stiffness of the model structure. Further studies are being performed to quantify soil and structure property uncertainties. The earthquake data collected in Hualien should provide additional understanding and validation of SSI effects and modeling.

5 ACKNOWLEDGMENT

Dr. W. S. Tseng and Dr. K. Lilhanand of International Civil Engineering Consultants provided valuable comments on analysis modeling and evaluation during the course of the study. Their contribution and cooperation are gratefully acknowledged.

REFERENCES

Kokusho, T. et al. 1993 Geotechnical Investigation in the Hualien Large Scale Seismic Test Project. *Proc. 12th SMiRT:* K03/4. pp. 85-90, Stuttgart: Germany

Morishita, H. et al. 1993. Forced Vibration Test of the Hualien Large Scale SSI Model. *Proc. 12th SMiRT:* K02/1. pp. 37-42. Stuttgart: Germany

Sugawara, Y. et al. 1995a. Forced Vibration Test of the Hualien Large Scale SSI Model (Part 2). *Proc. 13th SMiRT:* Porto Alegre: Brazil (Submitting)

Sugawara, Y. et al. 1995b. Correlation analysis for forced vibration test of the Hualien LSST Program. *Proc. 13th SMiRT:* Porto Alegre: Brazil (Submitting)

Tang, H. T. et al. 1991. The Hualien Large-Scale Seismic Test for Soil-Structure Interaction Research. *Proc. 11th SMiRT:* K04/04. pp. 18-23. Tokyo: Japan

Tang, H. T. & N. Nakamura 1995. Analysis of the Forced Vibration Test of the Hualien Large Scale Soil-Structure Interaction Model Using a Flexible Volume Substructuring Method. *Proc. ICONE-3:* Kyoto: Japan (Submitting)

The SASSI development team. 1988. SASSI USER'S MANUAL

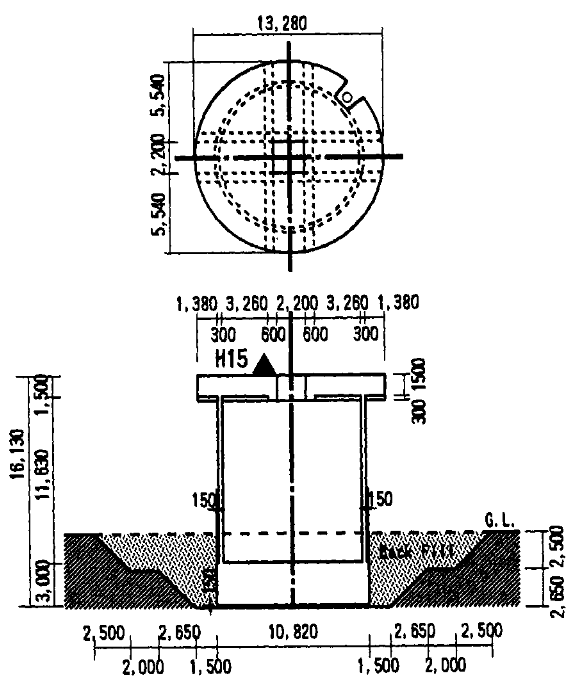

Figure 1 1/4-scale Containment Model in Hualien (unit:mm)

Table 1 Structure Property

Height (m)	Weight (t)	Rota-tional Inertia (tm²)	Case-A Ec (t/cm²)	Case-A I (m⁴)	Case-A An (m²)	Case-A As (m²)	Case-B Ec (t/cm²)	Case-B I (m⁴)	Case-B An (m²)	Case-B As (m²)
11.13	240	2780								
			288	1520	134	66.8	288	1520	134	134
9.63	274	3220								
			288	126	9.63	4.82	157	126	9.63	6.72
7.704	44.6	596								
			288	126	9.63	4.82	210	126	9.63	6.72
5.778	44.6	596								
			288	126	9.63	4.82	210	126	9.63	6.72
3.852	44.6	596								
			288	126	9.63	4.82	210	126	9.63	6.72
1.926	44.6	596								
			288	126	9.63	4.82	210	126	9.63	6.72
0.0	68.4	964								
			ν=0.16				ν=0.167			

Unit weight:2.4 ton/m3 Damping ratio:2% Ec:Young's modulus ν:Poisson's ratio
I:Geometrical moment of inertia An:Axial area As:Shear area

Table 2 Soil Property

	Case - A Vs	ν	ρ	h	Case - B Vs	ν	ρ	h
①	200	0.48	1.93	5	200	0.48	1.93	5
②	383	0.48	2.42	2	383	0.48	2.42	2
③	476	0.47	2.42	2	476	0.47	2.42	2
④	200	0.38	1.69	2	250	0.38	1.69	2
⑤	400	0.38	2.33	2	400	0.38	2.33	2
⑥	133	0.38	1.69	2	133	0.38	1.69	2
⑦	200	0.48	1.93	2	250	0.48	1.93	2
⑧	400	0.48	2.39	2	400	0.48	2.39	2
⑨	231	0.48	1.93	2	231	0.48	1.93	2

Vs:Shear wave velocity(m/sec)
ν:Poisson's ratio ρ:Unit weight(t/m³)
h:Damping ratio(%)

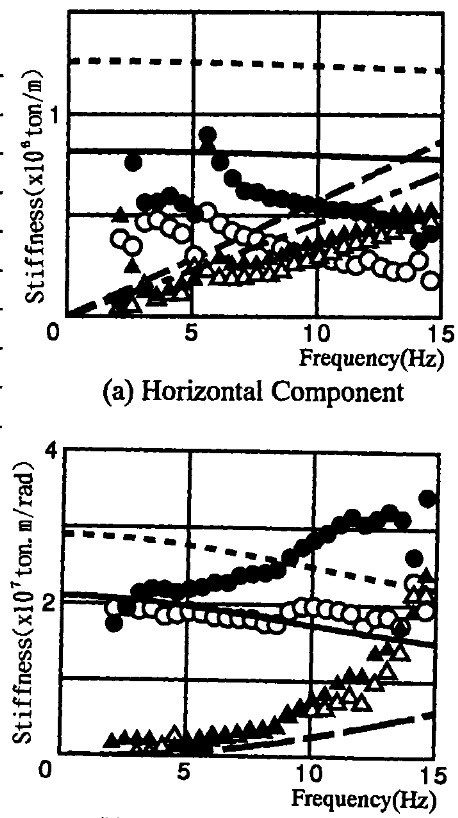

(a) Horizontal Component

(b) Rotational Component

—— line - A (Real Part)
-·-·- line - A (Imaginary Part)
······ line - B (Real Part)
— — line - B (Imaginary Part)
○ Back-calculated in D1 (Real Part)
△ Back-calculated in D1 (Imaginary Part)
● Back-calculated in D2 (Real Part)
▲ Back-calculated in D2 (Imaginary Part)

Figure 2 Impedance Function

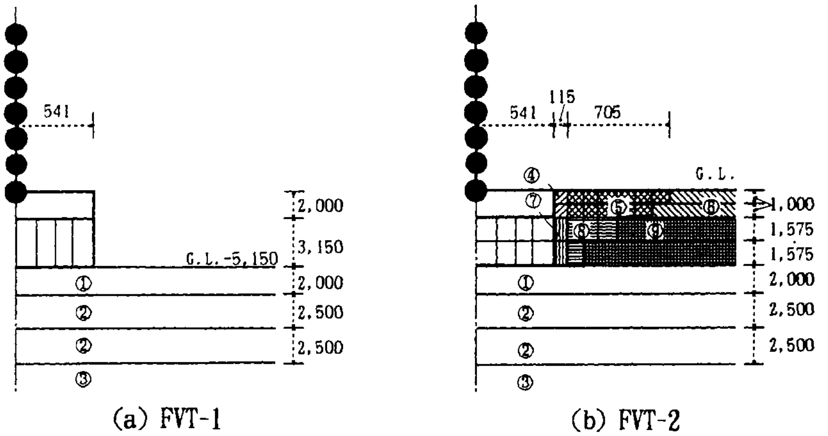

Figure 3 Analysis Model

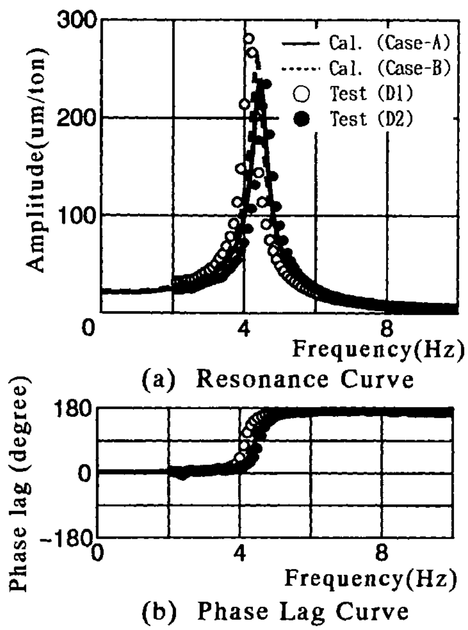

Figure 4 Roof Floor Excitation Result of FVT-1

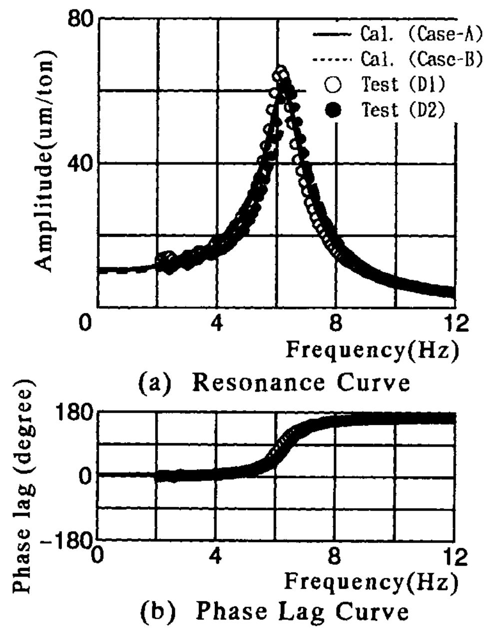

Figure 5 Roof Floor Excitation Results of FVT-2

Table 3 Analysis Results

Case		FVT-1 Peak Frequency (Hz)	FVT-1 Damping Factor (%)	FVT-1 Ratio(%) R	FVT-1 Ratio(%) S	FVT-1 Ratio(%) E	FVT-2 Peak Frequency (Hz)	FVT-2 Damping Factor (%)	FVT-2 Ratio(%) R	FVT-2 Ratio(%) S	FVT-2 Ratio(%) E
Case-A		4.44	4.3	69	12	19	6.20	9.8	64	10	26
Case-B		4.35	4.1	66	11	23	6.45	11.1	55	11	34
Test	D1	4.1	3.6	56	7	37.	6.1	8.2	57	7	36
Test	D2	4.6	3.7	66	11	23	6.3	8.2	52	8	40

R, S, E: Deformation ratio of rocking, sway and elastic components